The high-transmission photonic crystal heterostructure Y-branch waveguide operating at photonic band region

Ting-Hang Pei and Yang-Tung Huang

Citation: Journal of Applied Physics **109**, 034504 (2011); doi: 10.1063/1.3532048
View online: http://dx.doi.org/10.1063/1.3532048
View Table of Contents: http://scitation.aip.org/content/aip/journal/jap/109/3?ver=pdfcov
Published by the AIP Publishing

The high-transmission photonic crystal heterostructure Y-branch waveguide operating at photonic band region

Ting-Hang Pei and Yang-Tung Huang[a)]
Department of Electronics Engineering and Institute of Electronics, National Chiao Tung University, 1001 Ta-Hsueh Road, Hsinchu, 30010 Taiwan, Republic of China

(Received 11 May 2010; accepted 1 December 2010; published online 3 February 2011)

We design a high-efficiency two-dimensional photonic crystal (PhC) Y-branch waveguide formed as a heterostructure with two different triangular PhCs composed of air holes. At photonic-band frequency regions corresponding to circular equifrequency surfaces, the two PhCs could be taken as effective homogeneous media with effective refractive indices. A triangular coupler composed of the PhC is designed at the input port in order to divide the incident beam into two parts. The two parts finally propagate into different channels. A case demonstrated here shows that the total transmission of light passing through the Y-branch waveguide is about 91.2%. The propagation phenomena can be explained by the mechanism of total internal reflection very well. © *2011 American Institute of Physics*. [doi:10.1063/1.3532048]

I. INTRODUCTION

Photonic crystals (PhCs) are formed with dielectric periodic structures and exhibit new electromagnetic phenomena.[1,2] They show some properties analog to semiconductors, such as the photonic band structures (PBSs) including photonic passing bands and photonic band gaps (PBGs), and complicate dispersion relations. In analogous to the electron transport in semiconductors, the Bloch theorem is applied to describe electromagnetic waves propagating in the PhC very well.

Semiconductor heterostructures, such as the quantum wells[3] can confine electrons in the nanoscale region, combine at least two different materials. Recently, PhC heterostructures[4] like their semiconductor counterparts have been introduced and shown attractively optical features. Such as omnidirectional resonance modes can be generated in one-dimensional (1D) periodic PhC heterostructures stacked with alternate μ-negative and ε-negative materials;[5–7] the photonic multiple heterostructures consisting of different PhCs can be used to enlarge the nontransmission frequency range of PhCs.[8] Moreover, the confinement of the photonic envelope wave function in a two-dimensional photonic heterostructure quantum well implemented with quasiperiodic array of vertical-cavity surface emitting lasers as a model system has been discussed.[9] It is possible to control the characteristics of the photonic envelope wave functions, and control photonic states in quasiperiodic media.

The notion of localized states formed at PhC impurities or defects[1] has been utilized to guide light in waveguides.[10–13] Light could be confined and propagate in the waveguide efficiently even through sharp bends. The frequency of the propagation mode is chosen at the PBG region. Recently, a PhC heterostructure waveguide with PhC core surrounded by a uniform low-index material has been analyzed.[14] In that paper, the structure is similar to the conventional dielectric-slab waveguide, in which the mechanism of guiding light is the total internal reflection at the crystal-material interface. Each mode in this waveguide needs to satisfy the transverse resonance condition because of the extra transverse phase shift.[15] The frequency of light in the PhC defects waveguide needs to be operated within the PBG but the PhC heterostructure waveguide has no such limitation. Besides, the advantage of the PhC heterostructure waveguide is the core wide enough for efficiently coupling to conventional waveguides.

The PBS shows different optical responses when light propagates inside the PhC at different frequencies. The PhC can be taken as an effective anisotropic material that presents birefringence effect. It can also be taken as an effective homogeneous material with an effective dielectric constant under certain condition.[16] In this paper, we propose a PhC heterostructure waveguide combined two different PhCs possessing different effective dielectric constants. The PhC heterostructure waveguide is formed with a PhC core and PhC claddings. We not only show that the PhC heterostructure Y-branch waveguide is an optical high-transmission device but also show that the total internal reflection takes place at the interface of two PhCs. Especially, the operating frequency belongs to the photonic passing band. All light propagations in this paper are demonstrated by using the finite-difference time-domain (FDTD) method.[17]

II. CONCEPT AND DESIGN OF PHC HETEROSTRUCTURE Y-BRANCH WAVEGUIDE

A. Structure of the PhC heterostructure waveguide

We consider a two-dimensional PhC heterostructure Y-branch waveguide lying in the *x*-*y* plane as shown in Fig. 1. It is composed of air holes embedded into the low-index dielectric material in a triangular array with a lattice constant *a*. A triangular coupler made of the PhC, whose composition is the same as the core, is designed at the input port. It is utilized to couple light from the outside region into the PhC heterostructure waveguide. The triangular coupler used here is equivalent to a traditional prism composed of a dielectric

[a)]Electronic mail: huangyt@nctu.edu.tw.

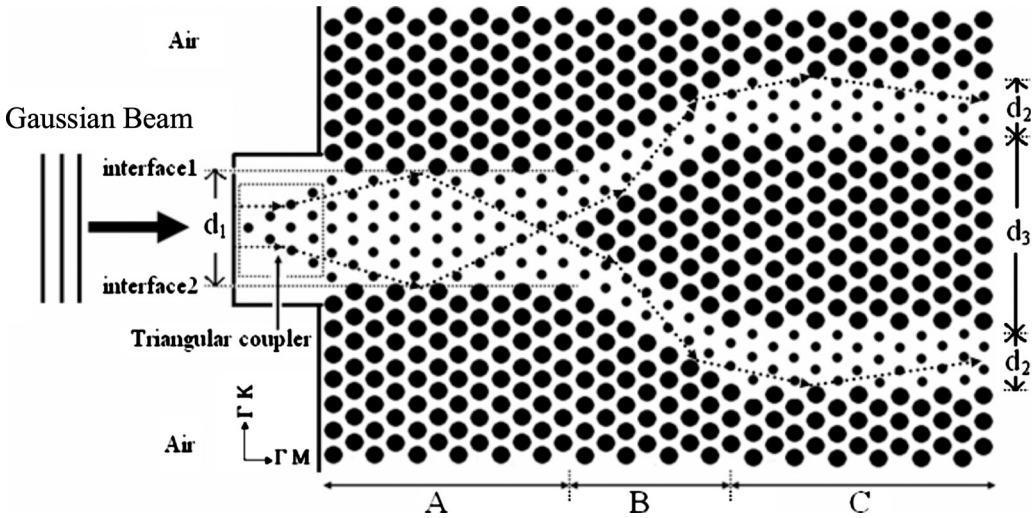

FIG. 1. The schematic of the PhC heterostructure Y-branch waveguide with a triangular coupler. The two dotted lines represent two interfaces and the extended rectangular region at the input represents the triangular coupler region. The arrows with dotted line denote the propagation direction when light propagates in the Y-branch waveguide.

material and each angle of it is 60°. The triangular coupler is a flexible design, whose effective refractive index can be varied with the radius of air holes. The triangular coupler can divide the incident Gaussian wave into two parts. The two divided waves go toward interface 1 and interface 2 (dotted lines) as shown in Fig. 1. Except for the triangular coupler, the whole structure is divided into three regions A, B, and C. Light meets different interfaces when propagates within A, B, and C regions. Light meets the interface along the ΓM direction in the A and C regions and meets the interface along the ΓK direction in the B region, respectively. The effective refractive index is chosen to be almost fixed for all propagation direction at the operating frequency. Light propagating inside the PhC heterostructure Y-branch waveguide is designed to obey the mechanism of the total internal reflection. So it needs to calculate the relation between n_d and n_c satisfying the total internal reflection in all regions, where n_d and n_c are the effective refractive indices for the claddings and core, respectively. In Fig. 1, the possible propagation processes satisfying the total internal reflections in all regions are simply shown by the ray traces with dotted-line arrows. In Fig. 2, the curve represents the limit of the relation between n_d and n_c. Values under the curve satisfy the condition of total internal reflection in all regions.

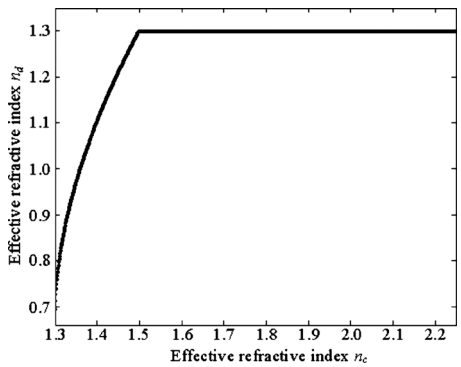

FIG. 2. The curve represents the limit of the relation between n_d and n_c. The values under the curve satisfy the total internal reflection in all A, B, and C regions.

B. Effective refraction index

The refractive angle of a light beam from one material into the PhC is determined by the equifrequency surfaces (EFSs) of light in the material and in the PhC. Each EFS corresponds to certain frequency. The group velocity is normal to the EFS at a certain wave vector and defined as $\vec{v}_g = \nabla_{\vec{k}}\omega$ in which $\vec{k}$ and ω are wave vector and frequency, respectively. Because the propagation direction is parallel to the group velocity, we can determine it in the PhC once $\vec{k}$ is given. According to the conservation rule, the incident and refractive wave vectors are continuous for the tangential components parallel to the interface. Given the incident wave vector with frequency and incident angle will determine the refractive wave vector and the refractive angle. By analyzing the EFS, we can find out the operating frequency at which optical response of the PhC is like that of a homogeneous material.

In our design as shown in Fig. 1, the background refractive indices of dielectric materials in the core and claddings are both 1.50. The radius r_1 of air holes in the core is $0.12a$ and the radius r_2 of air holes in the claddings is $0.42a$. The width of the core in the A region of the PhC heterostructure waveguide is d_1 and its length along the ΓM direction is L. The distance between two channels is d_3 in the C region. The width of each channel d_2 is equal to half d_1. From the calculation of EFSs in the first band, the shapes of EFSs are round the same as shapes of EFSs in homogeneous materials as shown in Fig. 3(a). When light is incident from air to the interface along the ΓK direction or the ΓM direction, we can define an effective refractive index N_{eff} from each EFS with the corresponding frequency as shown in Fig. 3(b). The upper and lower curves are the N_{eff}-frequency relations for r_1 and r_2, respectively. The radius of each EFS increases as the operating frequency increase, so each N_{eff} is positive defined

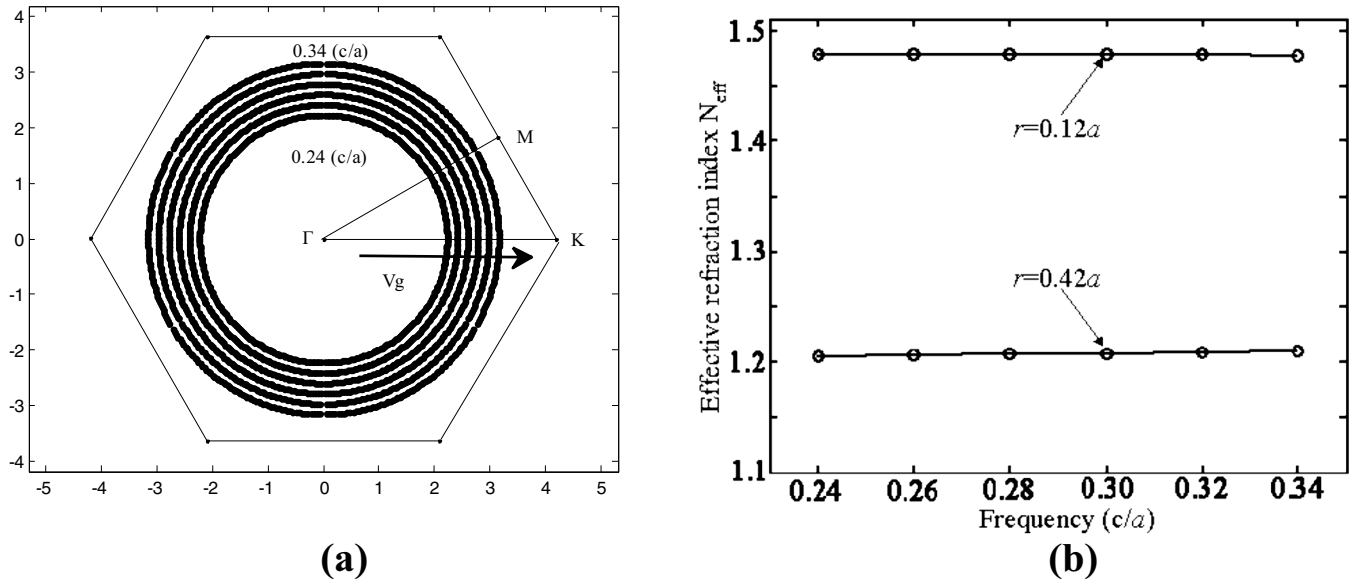

FIG. 3. (a) The EFSs for the radius r_1 of air holes. The frequencies of the inner and the outer circles are $0.24(c/a)$ and $0.34(c/a)$, respectively. (b) The N_{eff}-frequency relations in (a) for r_1 and r_2, respectively.

here. The operating frequency is chosen as $0.30(c/a)$. At this frequency, the $N_{\text{eff}}(n_c)$ for the core is 1.478 and the $N_{\text{eff}}(n_d)$ for claddings is 1.205. Both N_{eff} values are below the curve in Fig. 2 and simultaneously satisfy the condition of the total internal reflection. In Sec. III, we calculate transmissions of the PhC heterostructure Y-branch waveguide and show it is a high-transmission device.

C. The approximate wave in the PhC

The propagation wave in the PhC is the Bloch wave which satisfies the periodic condition. However, the round EFS also implies that the Bloch wave should be very close to the propagation wave in the effective medium with an effective refractive index N_{eff}. In the following, we calculate the Bloch wave in the PhC by using the plane-wave expansion method in order to verify the justification of the effective refractive index. The Bloch wave can be expressed as sum of all the Fourier series[18]

$$E_{z,\vec{k}n}(\vec{r}) = e^{i\vec{k}\cdot\vec{r}} \sum_{\vec{G}} E_{z,\vec{k}n}(\vec{G}) e^{i\vec{G}\cdot\vec{r}}, \tag{1}$$

where $\vec{k}$ is the wave vector in the first Brillouin zone, n is a band index, and $\vec{G}=\vec{G}_{pq}=p\vec{G}_1+q\vec{G}_2$ with integers p and q. The elementary lattice vectors are $\vec{a}_1=(a,0)$ and $\vec{a}_2=(a/2,\sqrt{3}a/2)$, and the elementary reciprocal lattice vectors in the k-space are $\vec{G}_1=2\pi/a(1,-1/\sqrt{3})$ and $\vec{G}_2=2\pi/a(0,2/\sqrt{3})$, respectively. According to PBSs in Figs. 4(a) and 4(b), where the first Brillouin zone is shown in Fig. 4(c), wave numbers of $\vec{k}$ in Eq. (1) are chosen as $k_1=0.4435\ (2\pi/a)$ and $k_2=0.3627\ (2\pi/a)$, respectively. These choices correspond to the frequency $0.30(c/a)$. Furthermore, wave number k can be expressed as $2\pi N_{\text{eff}}/a$ where N_{eff} are 1.478 and 1.205 for r_1 and r_2, respectively. When TM waves with frequency $0.30(c/a)$ propagate along the ΓM direction in PhCs with radii of r_1 and r_2, the real part of E_z fields are, respectively, shown in Figs. 5(a) and 5(b). These fields can be approximately described by Eq. (1) in which several co-

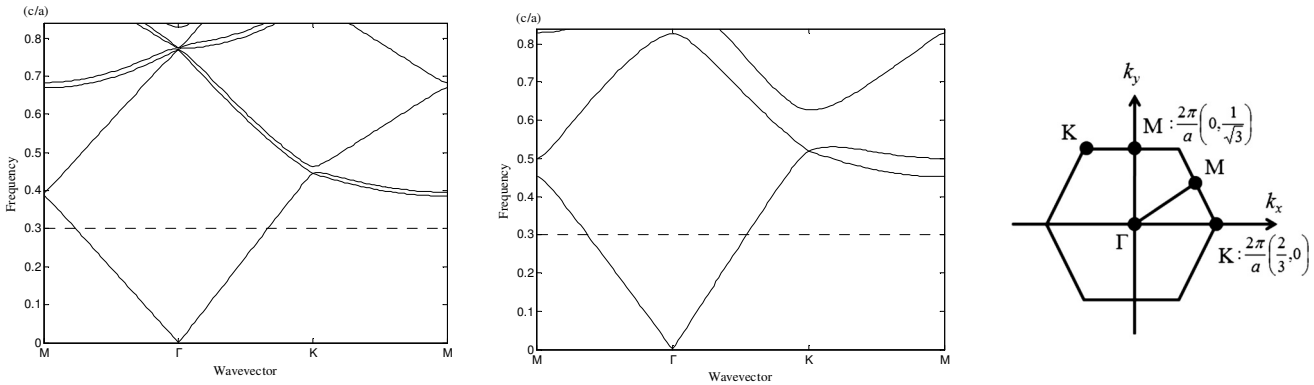

FIG. 4. (a) The PBS when the radius r is $0.12a$. (b) The PBS when the radius r is $0.42a$. (c) The first Brillouin zone of the triangular PhC.

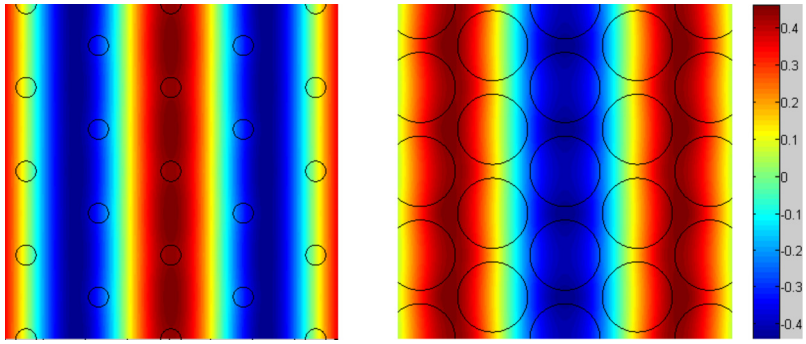

(a) (b)

FIG. 5. (Color online) (a) E_z field in the PhC the radius r is $0.12a$. (b) E_z field in the PhC the radius r is $0.42a$.

efficients more than 0.01 are included. The maximum one is the $\vec{G}_{00}$ term, which are 0.999 and 0.9934 for r_1 and r_2 cases, respectively. All higher ones are very small and less than 0.01 in the r_1 case. In the case of r_2, the other coefficients more than 0.01 are $\vec{G}_{-1-1}$, $\vec{G}_{0-1}$, and $\vec{G}_{10}$ terms which are -0.0298, -0.0160, and -0.160, respectively. So the waves $\phi^{(1)}_{\mathrm{PhC}}$ and $\phi^{(2)}_{\mathrm{PhC}}$ in these two PhCs can be approximately expressed as

$$\phi^{(1)}_{\mathrm{PhC}}(x,y) \approx Ae^{i\vec{k}_1\cdot\vec{r}} \times [0.999e^{i\vec{G}_{00}\cdot\vec{r}}] \approx \phi^{(1)}_{\mathrm{eff}} \times (x,y), \quad (r_1 \text{ case}), \tag{2}$$

$$\begin{aligned}\phi^{(2)}_{\mathrm{PhC}}(x,y) \approx{}& Ae^{i\vec{k}_2\cdot\vec{r}} \times [0.9934e^{i\vec{G}_{00}\cdot\vec{r}} - 0.0298e^{-i\vec{G}_{0-1}\cdot\vec{r}} \\ &+ 0.0160(e^{-i\vec{G}_{-1-1}\cdot\vec{r}} + e^{-i\vec{G}_{10}\cdot\vec{r}})] \approx \phi^{(2)}_{\mathrm{eff}}(x,y) \\ &\times [0.9934 - 0.0298e^{-i(4\pi/\sqrt{3}a)y} \\ &+ 0.0160(e^{-i(2\pi/a)(x+y/\sqrt{3})} \\ &+ e^{i(2\pi/a)(x-y/\sqrt{3})})], \quad (r_2 \text{ case}),\end{aligned} \tag{3}$$

where A is the constant amplitude. Because coefficients of $\vec{G}_{00}$ term in these two cases are at least 33 times larger than those of all higher ones, Eqs. (2) and (3) can be further simplified by dropping all higher terms. Finally, waves in these two PhCs are very close to those in two effective homogeneous media, that is, $\phi^{(1)}_{\mathrm{eff}}(x,y) = Ae^{i\vec{k}_1\cdot\vec{r}}$ and $\phi^{(2)}_{\mathrm{eff}}(x,y) = Ae^{i\vec{k}_2\cdot\vec{r}}$. It means that these two PhCs at frequency $0.30(c/a)$ can be much appropriately replaced with two effective homogeneous media of $N_{\mathrm{eff}}=1.478$ and $N_{\mathrm{eff}}=1.205$ as well as optical responses.

When TM waves with frequency $0.30(c/a)$ propagate along the ΓK direction in PhCs with radii of r_1 and r_2, E_z fields can be, respectively, approximated to

$$\begin{aligned}\phi^{(1)}_{\mathrm{PhC}}(x,y) \approx{}& Ae^{i\vec{k}_1\cdot\vec{r}} \times [0.999e^{i\vec{G}_{00}\cdot\vec{r}} - 0.0118(e^{-i\vec{G}_{-1-1}\cdot\vec{r}} \\ &+ e^{-i\vec{G}_{-10}\cdot\vec{r}})] \approx \phi^{(1)}_{\mathrm{eff}}(x,y) \times [0.999 - 0.0118 \\ &\times (e^{-i(2\pi/a)(x+y/\sqrt{3})} \\ &+ e^{-i(2\pi/a)(x-y/\sqrt{3})})], \quad (r_1 \text{ case}),\end{aligned} \tag{4}$$

$$\begin{aligned}\phi^{(2)}_{\mathrm{PhC}}(x,y) \approx{}& Ae^{i\vec{k}_2\cdot\vec{r}} \times [0.9934e^{i\vec{G}_{00}\cdot\vec{r}} - 0.0241(e^{-i\vec{G}_{-1-1}\cdot\vec{r}} \\ &+ e^{-i\vec{G}_{-10}\cdot\vec{r}})] \approx \phi^{(2)}_{\mathrm{eff}}(x,y) \times [0.999 - 0.0241 \\ &\times (e^{-i(2\pi/a)(x+y/\sqrt{3})} \\ &+ e^{-i(2\pi/a)(x-y/\sqrt{3})})], \quad (r_2 \text{ case}).\end{aligned} \tag{5}$$

Equations (4) and (5) can be also further simplified by the same reason mentioned above. Waves propagating along ΓK direction in these two PhCs can also be treated as plane waves propagating in two effective homogeneous media of $N_{\mathrm{eff}}=1.478$ and $N_{\mathrm{eff}}=1.205$. So the effective refraction index can perform the optical performance of the PhC very well.

III. TRANSMISSIONS OF THE PHC HETEROSTRUCTURE Y-BRANCH WAVEGUIDE

In order to investigate the transport phenomenon, the FDTD method is used to simulate light incident from the triangular coupler into the PhC heterostructure Y-branch waveguide. A TM-mode Gaussian beam with the electric field perpendicular to the x-y plane is lunched into the device. L and d_3 are chosen as $80\sqrt{3}a$ and $54a$, respectively. In our design, d_2 is equal to half d_1. Using these design parameters, we calculate transmissions of different d_1 values from $14a$ to $30a$ as shown in Fig. 6(a). The best transmission from the A region to the C region is about 45.6% at each output channel when d_1 is $28a$ and d_2 is $14a$. In advanced, we calculate the transmission of each output channel at different lengths of the A region from $50\sqrt{3}a$ to $320\sqrt{3}a$ when d_1 is $28a$ and d_2 is $14a$. The results are recorded in Fig. 6(b). We find the minimal transmission case takes place at $190\sqrt{3}a$. The second maximum transmission case takes place at $300\sqrt{3}a$. The period of the transmission between two successive maximum peaks is $220\sqrt{3}a$ in our calculations.

E_z field of the best transmission case is demonstrated in Fig. 7. It can be found that the triangular coupler divides incident beam into two parts at the input and then propagate toward two interfaces where total internal reflections take place. It is noticeable that the steady interface mode does not exist at interfaces 1 and 2, so no energy transfers from core region to the interface and energy is almost kept inside the waveguide. In the B region, total internal reflections take place explicitly that light reflects twice from the interfaces. When light enters into the C region, light propagates forwardly and is confined in the waveguide very well.

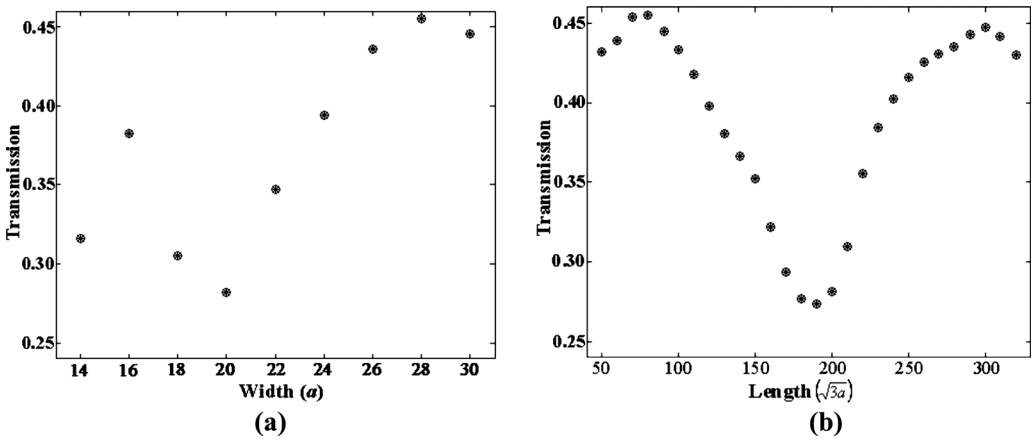

FIG. 6. The transmission of light incident from air into the PhC heterostructure Y-branch waveguide (a) when L is fixed at $80\sqrt{3}a$ and d_1 is changed from $14a$ to $30a$, (b) when d_1 is fixed at $28a$ and L is changed from $50\sqrt{3}a$ to $320\sqrt{3}a$.

A demonstration of the FDTD simulation at first minimal transmission is shown in Fig. 8. A lot of light leaking out from the B region results in energy loss and simultaneously decreases the transmission from the A region to the C region. Besides, total internal reflections are not satisfied in the C region in which some energy is also lost. The transmission from the A region to the C region is about 27.3% at each output channel. The transmission decreases 18.3% at each channel when the length increases from $80\sqrt{3}a$ to $190\sqrt{3}a$.

The second maximum transmission case at $300\sqrt{3}a$ is demonstrated in Fig. 9. Even light in the A region propagates through a distance almost four times longer than that of the first maximal transmission case, it is still confined in the waveguide very well. The transmission is close to 45%. Only 1.2% energy is lost when the length of A region increases from $80\sqrt{3}a$ to $300\sqrt{3}a$.

Finally, we investigate another high-efficiently transmission case by broadening the distance d_3. The length in the A region is still held at $80\sqrt{3}a$ and the widths d_1 and d_2 are fixed at $28a$ and $14a$, respectively. d_3 is chosen twice larger than that in Fig. 7, that is, $108a$. The field distribution is shown in Fig. 10. In the B region, the multiple total internal reflections take place explicitly. From FDTD calculation, the transmission is still close to 45%. Only 1.2% energy is lost when the distance between two channels is broadened from $54a$ to $108a$.

IV. COMPARISON OF THE GUIDING MECHANISMS BETWEEN THE PHC DEFECT WAVEGUIDE AND THE PHC HETEROSTRUCTURE WAVEGUIDE

A. PBG guiding

A lot of researches about PhC defect waveguides pay much attention on defect modes. It is well-known that frequencies of defect modes are within PBGs. Often, the PhC defect waveguide is created by removing or adding some specific pattern of air holes or rods which are used to guide light from one place to another. Generally speaking, most of electromagnetic field is localized in the core region and attenuates exponentially when enters into the cladding region formed by the PhC because the defect mode has a complex wave vector in it.

The PhC heterostructure waveguide use the mechanism of total internal reflection to transmit energy in the waveguide. If the incident angle at the interface between the core and claddings is smaller than the critical angle, energy will leak out from the core into claddings. On the contrary, energy transmitted in the PhC defect waveguide has nothing to do with the critical angle. It only depends on frequency of light whether or not locates within the PBG.

Jamois *et al.*[19] has given a review of the properties of silicon-based two-dimensional PhCs. The dielectric constant of silicon they used is 11.6. They have shown the guiding of TE mode in the PhC defect waveguide. Here we use the same structure to demonstrate an example of the guiding of TM mode in it. The structure of it formed by a triangular lattice of air holes where a row of air holes are removed along the ΓM direction is shown in Fig. 11(a). The lattice constant is a and the radius of all air holes is $0.43a$. The supercell method is used to calculate the PBS and defect

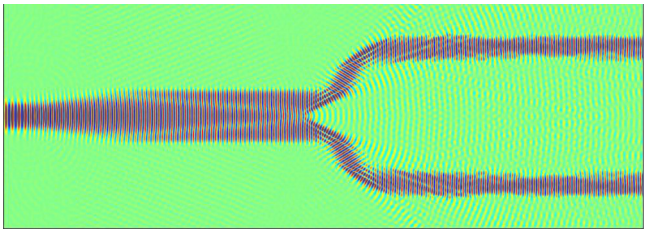

FIG. 7. (Color online) E_z field in the PhC heterostructure Y-branch waveguide when L, d_1, d_2, and d_3 are $80\sqrt{3}a$, $28a$, $14a$, and $54a$, respectively.

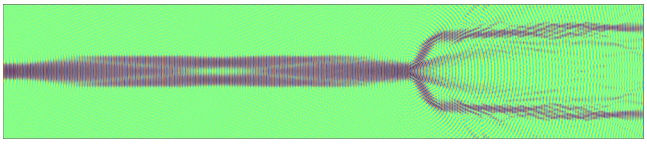

FIG. 8. (Color online) E_z field in the PhC heterostructure Y-branch waveguide where L, d_1, d_2, and d_3 are $190\sqrt{3}a$, $28a$, $14a$, and $54a$, respectively.

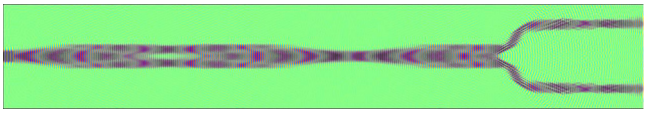

FIG. 9. (Color online) E_z field in the PhC heterostructure Y-branch waveguide where L, d_1, d_2, and d_3 are $300\sqrt{3}a$, $28a$, $14a$, and $54a$, respectively.

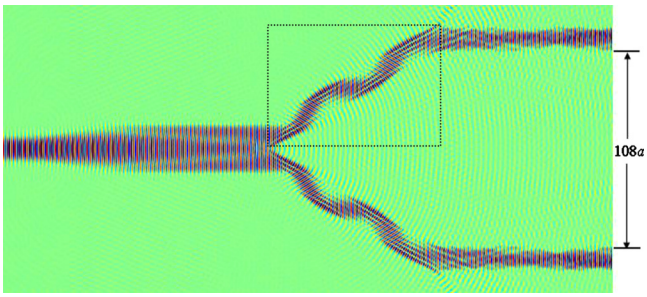

FIG. 10. (Color online) E_z field in the PhC heterostructure Y-branch waveguide where L, d_1, d_2, and d_3 are $80\sqrt{3}a$, $28a$, $14a$, and $108a$, respectively.

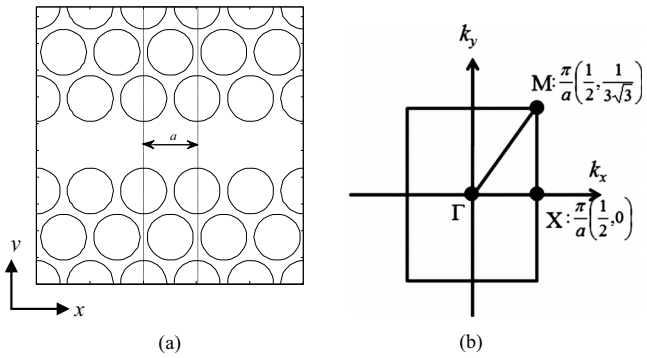

FIG. 11. (a) The supercell with size of $a \times 3\sqrt{3}a$ in the PhC removed a row of air hole. (b) The first Brillouin zone in the k-space. The band structures are calculated along M-Γ-X-M.

modes, where the supercell denoted as a rectangular region with area $a \times \sqrt{3}a$ is shown in Fig. 11(a). The first Brillouin zone in the k-space is shown in Fig. 11(b). Calculations of the PBS and defect modes along M-Γ-X-M are shown in Fig. 12(a). E_z field of a defect mode is shown in Fig. 12(b). Frequency of this defect mode corresponding to the star symbol in the PBG is $0.40(c/a)$. It can be investigated that most of E_z field is confined in the core region. The distance of transverse distribution is less than one air-hole width in the cladding region. It is not the case that total internal reflection takes place at the interface between a high-index medium and a low-index one. The defect mode propagates in the waveguide without considering the critical angle because it is meaningless here.

B. Index guiding

We have mentioned that the guiding mechanism in the PhC heterostructure waveguide is index guiding. In Sec II B, effective refraction indices are calculated from EFSs and used to replace with optical responses of the PhCs. It has been proved in Sec. II C that Bloch waves in the PhCs can approximate to waves in effective homogeneous media with effective refraction indices. From the viewpoint of effective refraction index, it is the case that the core of the PhC heterostructure waveguide is made of a high-index medium and the cladding of it is made of a low-index medium. Unlike the frequency of the defect mode within the PBG, the operating frequency of the wave in the PhC heterostructure waveguide is within the photonic conducting band where the wave vector of light is real in the PhC and light can propagate in it. So the mechanism of PBG guiding cannot use to explain the wave propagation in the PhC heterostructure waveguide.

In the following, we calculate the propagation directions of energy flow in one arm region enclosed by dashed-line rectangle in Fig. 10. It has been showed that the group ve-

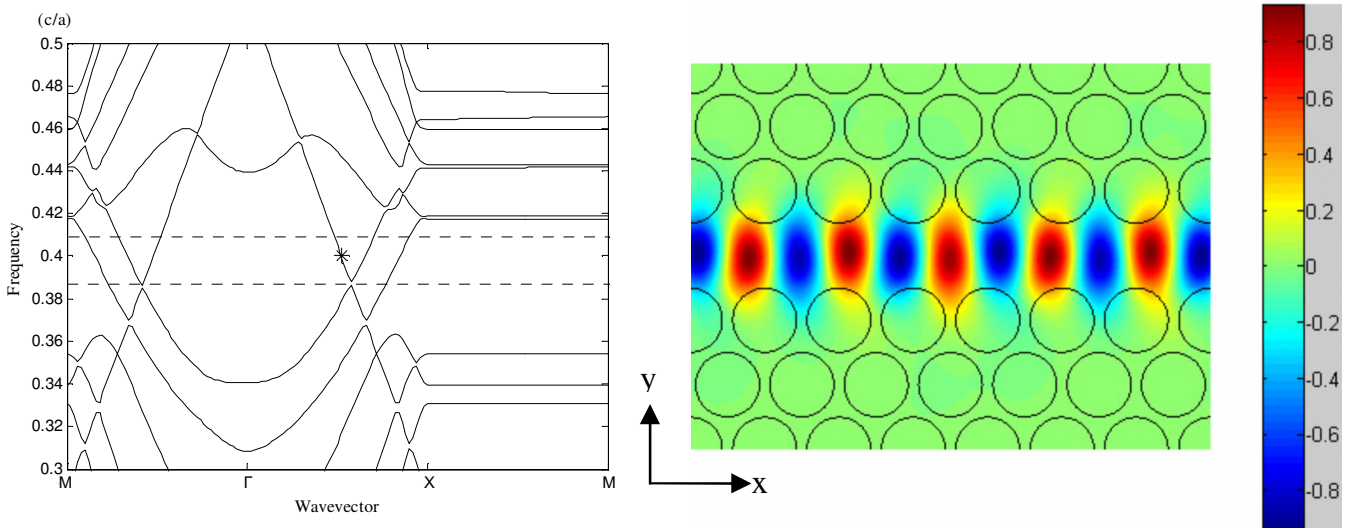

FIG. 12. (Color online) (a) Defect modes exist between 0.387 and $0.410(c/a)$ in the structure of Fig. 11(a), where a triangular array of air holes are embedded in the material with dielectric constant 11.6, and the radius r of all air holes is $0.43a$. The two horizontal lines denote the PBG edges. (a) E_z field is drawn along the PhC waveguide when the frequency of the defect mode is $0.40(c/a)$.

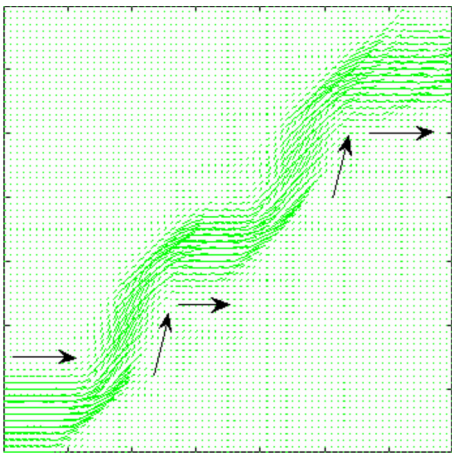

FIG. 13. (Color online) Directions of energy flow in one arm region enclosed by dashed-line rectangle in Fig. 10.

locity $\vec{v}_g$ is equal to the averaged energy velocity $\langle \vec{v}_e \rangle$ in a unit cell, that is, $\langle \vec{v}_e \rangle = \vec{v}_g = \nabla_{\vec{k}} \omega$.[20] $\langle \vec{v}_e \rangle$ is defined as

$$\langle \vec{v}_e \rangle = \frac{\frac{1}{S}\int \vec{P}_{\vec{k}} d\vec{r}_{\parallel}}{\frac{1}{S}\int U_{\vec{k}} d\vec{r}_{\parallel}} \equiv \frac{\langle \vec{P}_{\vec{k}} \rangle}{\langle U_{\vec{k}} \rangle}, \tag{6}$$

where S is the area of a unit cell and the integral range, $\vec{P}_{\vec{k}}$ is the time-averaged Poynting vector, and $U_{\vec{k}}$ is time-averaged energy density. The energy direction of each unit cell in this rectangle region is shown in Fig. 13. The green arrow orientation means the direction of averaged energy velocity in each unit cell. The length of each arrow also represents the magnitude of energy flow in each unit cell. The large black arrows show the trend of energy flow from region A to region C in the waveguide. Most of transmitted energy is confined in the core and total internal reflection of light takes place four times at the interface between the core and cladding. If we extend or reduce the length of region A, total internal reflection may not satisfy that some energy will leak out from the core into the cladding. It is obvious that some energy leaks out when length of region A increases from $80\sqrt{3}a$ to $190\sqrt{3}a$. In summary, the guiding mechanism of the wave propagation in the PhC heterostructure waveguide can be explained very well by Snell's law.

C. Transverse phase shift

From the ray-optic point of view,[21] one needs only Snell's law of total internal reflection to explain the propagating of light in a waveguide like our effective structure. Each mode in the waveguide can be derived by using geometric optics due to wave propagation in it can be represented by two plane waves. One of the plane waves may be considered as the incident wave, and the other may be treated as reflected one. They move in zigzag paths like waves propagating in the B region as shown in Fig. 10. However, the total internal reflection is only a necessary condition which is not sure whether all waves trapped in the core region constitute a mode. In order to establish a guided mode, all waves have to be in phase no matter how many times they reflect from two interfaces between core and claddings. A guided mode with propagation constants β and h, respectively, parallel to and perpendicular to the waveguide direction can thus be represented by plane waves traveling at an angle θ. The wave number in the core region is $k_0 n_c$ where k_0 is the wave number in vacuum. Then we obtain relations $\beta = k_0 n_c \sin\theta$ and $h = k_0 n_c \cos\theta$. According to the condition known as transverse resonance,[22] the net phase shift measured during a round trip, where a zigzag path forms from one interface to the other one and back again to original interface, must be a multiple of 2π. This leads to the condition,

$$2ht - 2\phi = 2m\pi, \tag{7}$$

where t is the thickness of the core region, m is the mode number, and ϕ is the phase shift upon total internal reflection at one of the interfaces. In our case, the phase shift ϕ can be expressed as

$$\phi = 2\tan^{-1}\frac{(n_c^2 \sin^2\theta - n_d^2)^{1/2}}{n_c \cos\theta}, \tag{8}$$

where n_c and the n_d are the effective refraction indices of core and claddings, respectively. We use the guided wave inside the B region in Fig. 10 to verify the condition of Eq. (7). The averaged propagation direction θ between two successive reflections shown in Fig. 10 is 60.4°. The thickness t of the core region is $7\sqrt{3}a$ so the ht is 5.311π. Substituting θ into Eq. (8), $\phi = 0.350\pi$ can be obtained. Next, ht and ϕ are both substituted into Eq. (7), we obtain $2ht - 2\phi = 9.92\pi$ which is very close to 10π. It figures out that the mode number m is 5. So the condition transverse resonance is satisfied in the heterostructure PhC waveguide.

V. CONCLUSION

In conclusion, in the case of our design, the operating frequency in the PhC heterostructure Y-branch waveguide is not at the PBG region but belongs to the photonic band region. The mechanisms of PBG guiding and index guiding are different and discussed in detail. The guided mechanism of the PhC heterostructure waveguide can be explained by total internal reflection in the waveguide. Even the two PhCs are grating structures, light almost obeys total internal reflection at each interface. Generally speaking for dielectric PhCs, the frequency region of photonic bands belonging to our case is often much larger than that of PBGs. So the usable frequency regions for our device are more than that for the PhC defect waveguide guiding light at the PBG regions. We also have more choices for designing a PhC heterostructure waveguide due to flexible values of the n_d and n_c. Finally, the results also show the fine way to use PhCs as effective media corresponding to circular EFSs, which will enrich the optical device design in the future.

ACKNOWLEDGMENTS

We are grateful to Dr. C. M. Kwei for offering valuable comments on this work.

[1]S. John, Phys. Rev. Lett. **58**, 2486 (1987).
[2]A. Z. Genack and N. Garcia, Phys. Rev. Lett. **66**, 2064 (1991).
[3]J. Piprek, *Semiconductor Optoelectronic Devices Introduction to Physics and Simulation* (Academic, San Diego, 2003).
[4]E. Istrate and E. H. Sargent, Rev. Mod. Phys. **78**, 455 (2006).
[5]Y. H. Chen, J. W. Dong, and H. Z. Wang, J. Opt. Soc. Am. B **23**, 2237 (2006).
[6]D. R. Fredkin and A. Ron, Appl. Phys. Lett. **81**, 1753 (2002).
[7]A. Alù and N. Engheta, IEEE Trans. Antennas Propag. **51**, 2558 (2003).
[8]C. Zhang, F. Qiao, J. Wan, and J. Zi, J. Appl. Phys. **87**, 3174 (2000).
[9]G. Guerrero, D. L. Boiko, and E. Kapon, Opt. Express **12**, 4922 (2004).
[10]A. Mekis, J. C. Chen, I. Kurland, S. Fan, P. R. Villeneuve, and J. D. Joannopoulos, Phys. Rev. Lett. **77**, 3787 (1996).
[11]A. Mekis, S. Fan, and J. D. Joannopoulos, Phys. Rev. B **58**, 4809 (1998).
[12]Z.-Y. Li and K.-M. Ho, Phys. Rev. B **68**, 045201 (2003).
[13]E. Moreno, D. Erni, and C. Hafner, Phys. Rev. E **66**, 036618 (2002).
[14]X. Yu, W. T. Lau, and S. Fan, Opt. Lett. **31**, 742 (2006).
[15]C. R. Pollock, *Fundamentals of Optoelectronics* (Irwin, Homewood, 1995).
[16]M. Notomi, Phys. Rev. B **62**, 10696 (2000).
[17]A. Taflove and S. C. Hagness, *Computational Electrodynamics* (Artech House, Norwood, 2000).
[18]K. Sokoda, *Optical Properties of Photonic Crystals*, 2nd ed. (Springer, Berlin, 2005).
[19]C. Jamois, R. B. Wehrspohn, L. C. Andreani, C. Hermann, O. Hess, and U. Gosele, Photonics Nanostruct. Fundam. Appl. **1**, 1 (2003).
[20]A. Yariv and P. Yeh, *Optical Waves in Crystals* (Wiley, New York, 1984).
[21]R. G. Hunsperger, *Integrated Optics: Theory and Technology*, 3rd ed. (Springer, Berlin, 1992).
[22]W. H. Hyat, Jr. and H. A. Buck, *Engineering Electromagnetics*, 6th ed. (McGraw-Hill, New York, 2001).